

# Electrical properties of $(\text{Na}_2\text{O})_{35.7}(\text{RE}_2\text{O}_3)_{7.2}(\text{SiO}_2)_{57.1}$ (RE = Y, Sm, Gd, Dy, Ho, Er and Yb) glasses and ceramics

Susumu Nakayama<sup>a,\*</sup>, Taro Asahi<sup>b</sup>, Hajime Kiyono<sup>c</sup>, Yan Lin Aung<sup>a</sup>, Masatomi Sakamoto<sup>d</sup>

<sup>a</sup> Department of Applied Chemistry and Biotechnology, Niihama National College of Technology, 7-1 Yagumo-cho, Niihama 792-8580, Japan

<sup>b</sup> Department of Materials Engineering, Niihama National College of Technology, Niihama 792-8580, Japan

<sup>c</sup> Division of Material Science and Engineering, Graduate School of Engineering, Hokkaido University, Sapporo 060-8628, Japan

<sup>d</sup> Department of Material and Biological Chemistry, Faculty of Science, Yamagata University, Yamagata 990-8560, Japan

Received 8 January 2005; received in revised form 28 February 2005; accepted 12 March 2005

Available online 17 May 2005

## Abstract

Fifteen kinds of sodium rare earth silicate glasses and ceramics with  $(\text{Na}_2\text{O})_{35.7}(\text{RE}_2\text{O}_3)_{7.2}(\text{SiO}_2)_{57.1}$  (RE = Y, Sm, Gd, Dy, Ho, Er and Yb) composition were synthesized from a mixture of  $\text{Na}_2\text{CO}_3$ ,  $\text{RE}_2\text{O}_3$  and  $\text{SiO}_2$ . The densities of the glasses were in fairly good agreement with the theoretical densities and were 0.2–0.41  $\text{g cm}^{-3}$  larger than those of the polycrystalline ceramics. The conductivities of the glasses are 1–2 orders lower than those of the ceramics and the highest electrical conductivity was achieved for the Yb ceramic sample with the smallest ion radius of  $\text{RE}^{3+}$ . The electromotive force, EMF, of the potentiometric  $\text{CO}_2$  gas sensors using  $(\text{Na}_2\text{O})_{35.7}(\text{Y}_2\text{O}_3)_{7.2}(\text{SiO}_2)_{57.1}$  glass and ceramic increased linearly with an increase in the logarithm of  $\text{CO}_2$  partial pressure, in accordance with Nernst's law. It was suggested from the slope of Nernst's equation that the two electron-transfer reaction associated with the carbon dioxide molecule takes place at the detection electrode above 450 °C.

© 2005 Elsevier Ltd. All rights reserved.

**Keywords:** Electrical conductivity; Silicate; Sensor; Glass; Nernst law

## 1. Introduction

$\text{Na}^+$  ionic conducting ceramics such as  $\beta''\text{-Al}_2\text{O}_3$  ( $4.2 \times 10^{-2} \text{ S cm}^{-1}$  at 200 °C) and  $\text{Na}_3\text{Zr}_2\text{Si}_2\text{PO}_{12}$  ( $6.7 \times 10^{-2} \text{ S cm}^{-1}$  at 200 °C) have been reported and some of these ceramics have been utilized as electrolyte-materials in Na–S cells and carbon dioxide gas sensors.<sup>1–3</sup> Sodium silicate ceramics,  $\text{Na}_5\text{RESi}_4\text{O}_{12}$  (RE = Sc, Y, Sm, Gd, Tb, Dy, Ho, Er, Tm, Yb and Lu), reported by Shannon et al.<sup>4</sup> are also known as rare earth containing ceramics which exhibit high  $\text{Na}^+$  ionic conduction ( $10^{-2} \text{ S cm}^{-1}$  at 200 °C). Generally, dense ionic conductors are desirable for the development of chemical sensor materials. As the result of the screening process for well compacted conductive  $\text{Na}^+$  ion solid electrolytes, we reported that the

$(\text{Na}_2\text{O})_{35.7}(\text{RE}_2\text{O}_3)_{7.2}(\text{SiO}_2)_{57.1}$  (RE = Y, Sm, Gd, Dy, Ho, Er and Yb) glasses are dense.<sup>5,6</sup> Furthermore, glasses have some advantages in terms of high chemical durability due to the absence of grain boundaries and the easy shaping and mechanical processing. In this work, electrical properties of the glass and ceramic with  $(\text{Na}_2\text{O})_{35.7}(\text{RE}_2\text{O}_3)_{7.2}(\text{SiO}_2)_{57.1}$  composition were investigated, along with the response characteristics of the potentiometric  $\text{CO}_2$  gas sensor in which  $(\text{Na}_2\text{O})_{35.7}(\text{Y}_2\text{O}_3)_{7.2}(\text{SiO}_2)_{57.1}$  glass or ceramic was used as a solid electrolyte.

## 2. Experimental

### 2.1. Sample preparation

Glass samples of  $(\text{Na}_2\text{O})_{35.7}(\text{RE}_2\text{O}_3)_{7.2}(\text{SiO}_2)_{57.1}$  (RE = Y, Sm, Gd, Dy, Ho, Er and Yb) were prepared from

\* Corresponding author. Tel.: +81 897 37 7786; fax: +81 897 37 7842.  
E-mail address: [nakayama@chem.niihama-nct.ac.jp](mailto:nakayama@chem.niihama-nct.ac.jp) (S. Nakayama).

$\text{Na}_2\text{CO}_3$  and  $\text{SiO}_2$ , and  $\text{RE}_2\text{O}_3$  (99.9% purity) powders. They were mixed in the molar ratio of  $\text{Na}_2\text{CO}_3:\text{RE}_2\text{O}_3:\text{SiO}_2 = 35.7:7.2:57.1$ , and then melted in a platinum crucible at  $1350^\circ\text{C}$  for 1 h in an air atmosphere. The melted sample was quenched on an iron plate, molded with pressing, and annealed at  $500^\circ\text{C}$  to prevent distortion and cracking. Ceramic samples were prepared in the same molar ratio as the glass samples, using each carbonate or oxide component. Powders were mixed in ethanol in a ball-mill using  $\text{Y}_2\text{O}_3$  stabilized zirconia balls and plastic pot, dried and calcined in air at  $800^\circ\text{C}$  for 2 h. The resultant powders were ball milled into fine powders. Dry powders were pressed at 100 MPa into disc and sintered in air at  $1250^\circ\text{C}$  for 2 h.

## 2.2. Measurements

The density was measured by the Archimedes method. The microstructures were observed by scanning electron microscopy (SEM, Hitachi X-560). The glass transition temperature ( $T_g$ ), the crystallization temperature ( $T_c$ ) and the melting temperature ( $T_m$ ) were measured by the differential thermal analysis (DTA, Rigaku TG8110) of the ground glass powder (200 mg) at a heating rate of  $10^\circ\text{C min}^{-1}$  in an air stream ( $50\text{ cm}^3\text{ min}^{-1}$ ). The formation of glass phase and the crystallization were confirmed by powder X-ray diffraction analysis (XRD, Rigaku MiniFlex). The  $^{23}\text{Na}$  MAS NMR spectra of  $(\text{Na}_2\text{O})_{35.7}(\text{Y}_2\text{O}_3)_{7.2}(\text{SiO}_2)_{57.1}$  glass and ceramic were recorded on a Bruker MSL-300 spectrometer. Sample spinning rate was 12 kHz. Repetition time of 4 s was employed. Chemical shifts were referenced to an aqueous NaCl solution. The electrical conductivities were measured in the temperature range of  $200\text{--}550^\circ\text{C}$  and in the frequency range of 100 Hz to 10 MHz with an impedance analyzer HP4194A on samples with Pt electrodes on both sides.

Both  $(\text{Na}_2\text{O})_{35.7}(\text{Y}_2\text{O}_3)_{7.2}(\text{SiO}_2)_{57.1}$  glass and ceramic were used as ionic conductors in the solid state cells of the  $\text{CO}_2$  sensor. The diameter and thickness of the discs after sintering were 8 and 2 mm, respectively. One side of a disc was coated with Pt paste and the other side with Au paste, and annealed at  $400^\circ\text{C}$ . Pt wires were connected to both sides of the disc. The Au detection electrode was immersed in an aqueous solution of  $\text{Na}_2\text{CO}_3$  and then dried to obtain the solid electrode. The sensor was fixed on one end of an alumina pipe with a glass cement so that the Pt counter electrode was located inside the pipe (see Fig. 1). The response characteristics of the sensors were measured for standard  $\text{CO}_2$  gases under the partial pressures of  $1 \times 10^0$  Pa,  $1 \times 10^1$  Pa,  $1 \times 10^2$  Pa and  $1 \times 10^3$  Pa, which were prepared by diluting given amounts of  $\text{CO}_2$  with synthetic air ( $<2 \times 10^{-1}$  Pa  $\text{CO}_2$ ) (Sumitomo-Seika Inc.). Measurements were performed by passing the  $\text{CO}_2$  gases through the detection electrode side of the sensors at the flow rate of  $50\text{ cm}^3\text{ min}^{-1}$ . The electromotive force, EMF, was measured using an Advantest TR8652 electrometer.

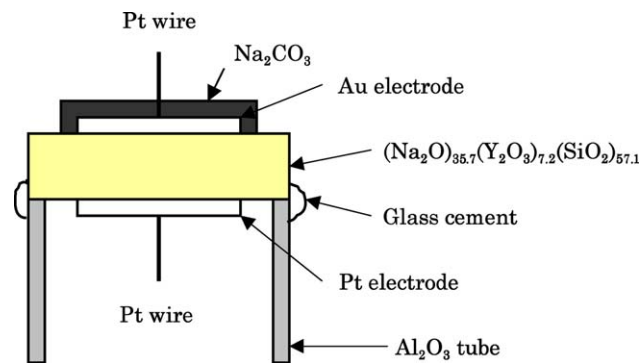


Fig. 1. Schematic view of  $\text{CO}_2$  gas sensors.

## 3. Results and discussion

### 3.1. Density

All the prepared glasses were transparent and homogeneous. The XRD pattern showed only a halo pattern near  $2\theta = 30^\circ$ , confirming the absence of crystalline phases. The color of each glass and ceramic depended on the kind of rare earth ion: colorless for the Gd, Dy, Y and Yb samples, pale yellow for the Sm sample, greenish yellow for the Ho sample and pink for the Er sample. As shown in Fig. 2, the densities of glasses were  $0.2\text{--}0.4\text{ g cm}^{-3}$  larger than those of ceramics. The density increased with increasing atomic weight of RE. The lower densities of ceramics can be understood from the microstructure of  $(\text{Na}_2\text{O})_{35.7}(\text{Y}_2\text{O}_3)_{7.2}(\text{SiO}_2)_{57.1}$  ceramic shown in Fig. 3. The sintering does not progress very well

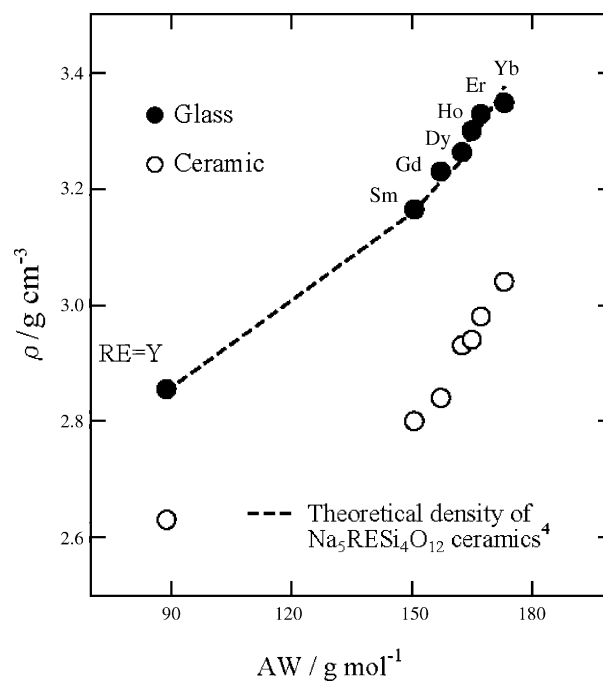


Fig. 2. Relationship between the atomic weight and the density of  $(\text{Na}_2\text{O})_{35.7}(\text{RE}_2\text{O}_3)_{7.2}(\text{SiO}_2)_{57.1}$  glasses and ceramics.

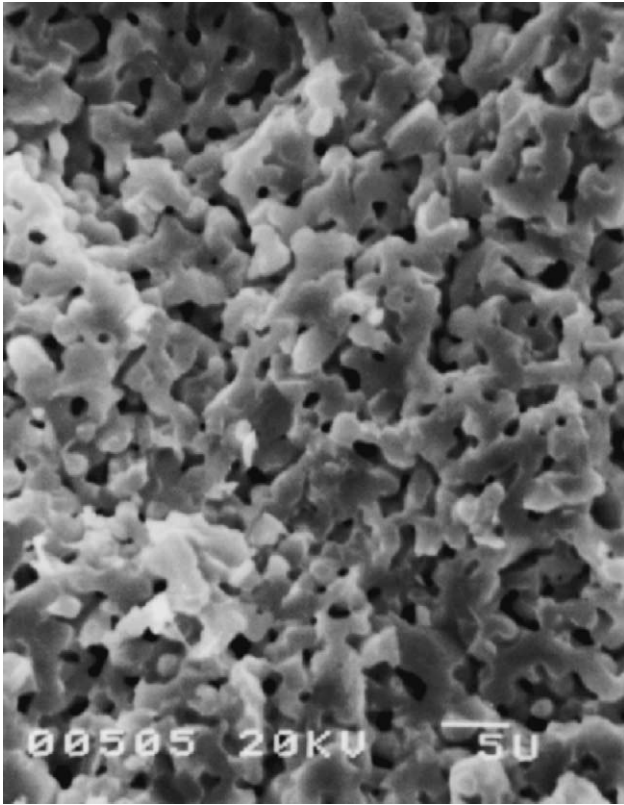


Fig. 3. SEM photograph of the microstructure of  $(\text{Na}_2\text{O})_{35.7}(\text{Y}_2\text{O}_3)_{7.2}(\text{SiO}_2)_{57.1}$  ceramic.

and many pores are observed. This was also the case for other  $(\text{Na}_2\text{O})_{35.7}(\text{RE}_2\text{O}_3)_{7.2}(\text{SiO}_2)_{57.1}$  ceramics.

### 3.2. DTA

The DTA patterns of  $(\text{Na}_2\text{O})_{35.7}(\text{RE}_2\text{O}_3)_{7.2}(\text{SiO}_2)_{57.1}$  glasses were essentially similar to each other. Fig. 4 shows the DTA curve of  $(\text{Na}_2\text{O})_{35.7}(\text{Y}_2\text{O}_3)_{7.2}(\text{SiO}_2)_{57.1}$  glasses as a typical result. A broad endothermic peak ( $T_g$ ) due to the glass transition was observed around 420 °C. Exothermic

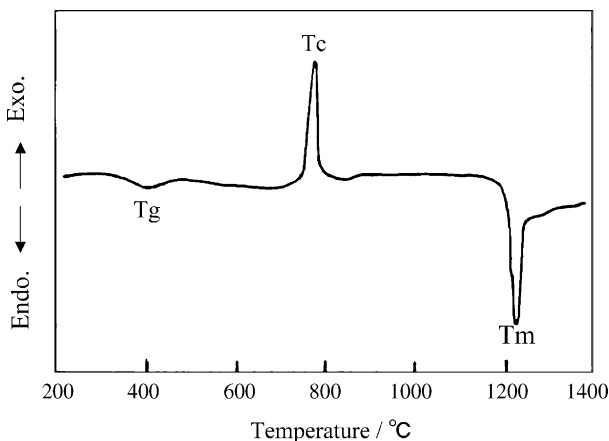


Fig. 4. DTA curve of  $(\text{Na}_2\text{O})_{35.7}(\text{Y}_2\text{O}_3)_{7.2}(\text{SiO}_2)_{57.1}$  glass.

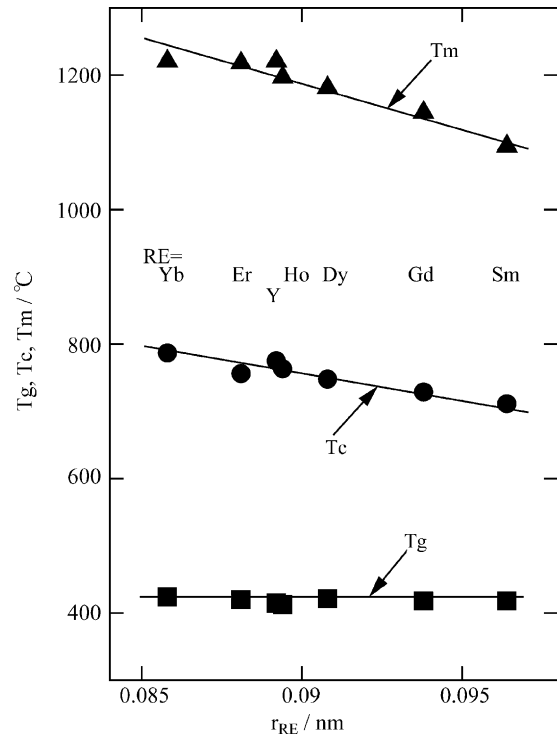


Fig. 5. Relationship between the ionic radius of  $\text{RE}^{3+}$  and the glass transition temperature ( $T_g$ ), the crystallization temperature ( $T_c$ ) and the crystal melting temperature ( $T_m$ ) of  $(\text{Na}_2\text{O})_{35.7}(\text{RE}_2\text{O}_3)_{7.2}(\text{SiO}_2)_{57.1}$  glasses.

and endothermic sharp peaks ( $T_c$  and  $T_m$ ) due to the crystallization and the melting of crystal appeared around 780 and 1220 °C, respectively. Fig. 5 shows the relationship between the ionic radius of  $\text{RE}^{3+}$  and temperatures of glass transition ( $T_g$ ), crystallization ( $T_c$ ) and melting of crystal ( $T_m$ ).  $T_c$  and  $T_m$  linearly decreased as ionic radius of  $\text{RE}^{3+}$  increased, whereas  $T_g$  was little affected by the kind of RE. All of samples crystallized around 800 °C, which is a bit higher than  $T_c$ , showed XRD patterns very similar to that of  $(\text{Na}_2\text{O})_{35.7}(\text{RE}_2\text{O}_3)_{7.2}(\text{SiO}_2)_{57.1}$  ceramics with a hexagonal structure.<sup>7,8</sup>

### 3.3. NMR

$^{23}\text{Na}$  NMR spectra of  $(\text{Na}_2\text{O})_{35.7}(\text{Y}_2\text{O}_3)_{7.2}(\text{SiO}_2)_{57.1}$  glass and ceramic are shown in Fig. 6. Only one peak marked as an arrow was observed for the glass. The spectral simulation suggested that the  $\text{Na}^+$  ions in the glass are statistically located at subtly different sites, which cannot be distinguished on the NMR time scale. On the other hand, the ceramic exhibited at least three peaks, (I)–(III). From the chemical shift, peak (II) is assignable to the  $\text{Na}^+$  ions, the site of which may be the same as that of  $\text{Na}^+$  ions in the glass. Peaks (I) and (III) are assigned to the  $\text{Na}^+$  ions which are located at the different sites from those of  $\text{Na}^+$  ions responsible for peak (II). Of these three sites, the crystallinity of the  $\text{Na}^+$ -site corresponding to peak (III) is reasonably thought to be the highest, because the peak (III) is less broadened compared to the other two peaks.

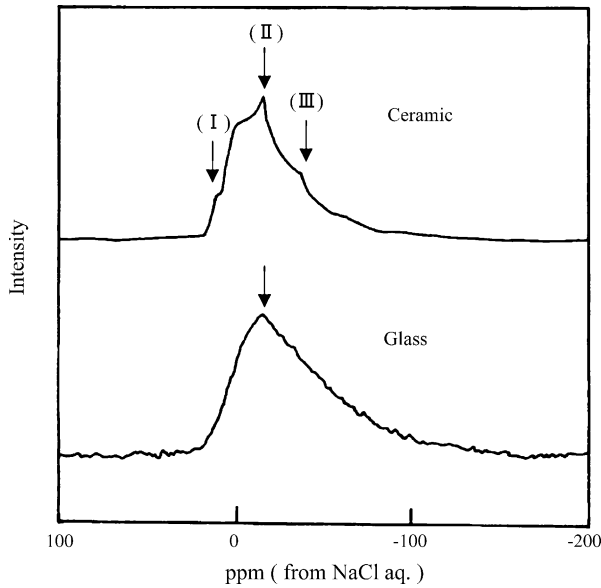


Fig. 6.  $^{23}\text{Na}$  MAS NMR spectra of  $(\text{Na}_2\text{O})_{35.7}(\text{Y}_2\text{O}_3)_{7.2}(\text{SiO}_2)_{57.1}$ .

### 3.4. Conductivity

The conductivities ( $\sigma$ ) of  $(\text{Na}_2\text{O})_{35.7}(\text{RE}_2\text{O}_3)_{7.2}(\text{SiO}_2)_{57.1}$  glasses and ceramics were measured in the range of 200–550 °C by complex impedance analysis. Typical Arrhenius plots of  $\log(\sigma T)$  versus  $1/T$  for  $(\text{Na}_2\text{O})_{35.7}(\text{Y}_2\text{O}_3)_{7.2}(\text{SiO}_2)_{57.1}$  glass and ceramic are shown in Fig. 7. Conductivities for glass were  $1.3 \times 10^{-4} \text{ S cm}^{-1}$  at 200 °C,  $1.3 \times 10^{-3} \text{ S cm}^{-1}$  at 300 °C and  $3.5 \times 10^{-3} \text{ S cm}^{-1}$  at 350 °C. The conductivity at 300 °C is comparable to that ( $1.2 \times 10^{-3} \text{ S cm}^{-1}$  at 300 °C) of the  $(\text{Na}_2\text{O})_{37.9}(\text{Y}_2\text{O}_3)_{7.6}(\text{SiO}_2)_{54.5}$  glass reported by Alexander and Riley.<sup>9,10</sup> The

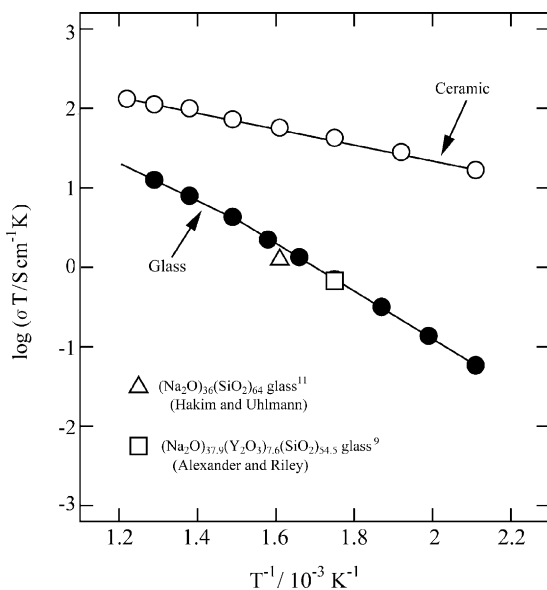


Fig. 7. Temperature dependence of conductivity for  $(\text{Na}_2\text{O})_{35.7}(\text{Y}_2\text{O}_3)_{7.2}(\text{SiO}_2)_{57.1}$  glass and ceramic.

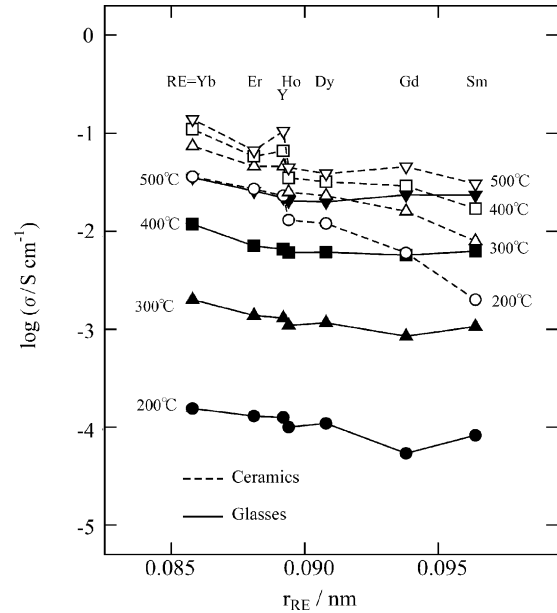


Fig. 8. Relationship between the ionic radius of  $\text{RE}^{3+}$  and the conductivities of  $(\text{Na}_2\text{O})_{35.7}(\text{RE}_2\text{O}_3)_{7.2}(\text{SiO}_2)_{57.1}$  glasses and ceramics.

conductivity of the glass is one to three orders lower than that of the ceramic. Shannon et al.<sup>4</sup> have reported that the conductivity of  $\text{Na}_5\text{RESi}_4\text{O}_{12}$  ceramic is about three orders higher than that of  $\text{Na}_2\text{Si}_2\text{O}_5$  ceramic. However, the present  $(\text{Na}_2\text{O})_{35.7}(\text{Y}_2\text{O}_3)_{7.2}(\text{SiO}_2)_{57.1}$  glass gave a conductivity similar to that ( $2 \times 10^{-3} \text{ S cm}^{-1}$  at 350 °C) of  $(\text{Na}_2\text{O})_{36}(\text{SiO}_2)_{64}$  glass reported by Hakim and Uhlmann,<sup>11</sup> indicating that there is no enhancement of conductivity by the addition of  $\text{Y}_2\text{O}_3$  to  $(\text{Na}_2\text{O})_{36}(\text{SiO}_2)_{64}$  glass. Conductivities of  $(\text{Na}_2\text{O})_{35.7}(\text{RE}_2\text{O}_3)_{7.2}(\text{SiO}_2)_{57.1}$  glasses and ceramics are plotted against ionic radius of  $\text{RE}^{3+}$  in Fig. 8. The conductivity slightly decreased with increasing ionic radius of  $\text{RE}^{3+}$ : in the series of  $(\text{Na}_2\text{O})_{35.7}(\text{RE}_2\text{O}_3)_{7.2}(\text{SiO}_2)_{57.1}$  materials prepared in this work, samples of  $\text{RE} = \text{Yb}$  showed the highest conductivity for both glass and ceramic.

### 3.5. Response characteristic as $\text{CO}_2$ gas sensor

Figs. 9 and 10 show the dependence of EMF on the logarithm of  $\text{CO}_2$  partial pressure,  $\log P_{\text{CO}_2}$ , for the  $(\text{Na}_2\text{O})_{35.7}(\text{Y}_2\text{O}_3)_{7.2}(\text{SiO}_2)_{57.1}$  glass and ceramic, respectively. The EMF decreased with increasing  $\log P_{\text{CO}_2}$  at each temperature, and the plots of EMF versus  $\log P_{\text{CO}_2}$  obeyed the Nernst equation. In the present apparatus designed so that the counter electrode is shielded from the detected gas, almost constant potential was obtained at a given temperature. This indicates that the number of electron transferred at the detection electrode can be estimated from the slope of the straight lines in Figs. 9 and 10 as the EMF is changed by the potential at the detection electrode. The electron number transferred was estimated as 2 above 450 °C.

The response mechanism of the present  $\text{CO}_2$  gas sensor was investigated. The counter electrode was always exposed

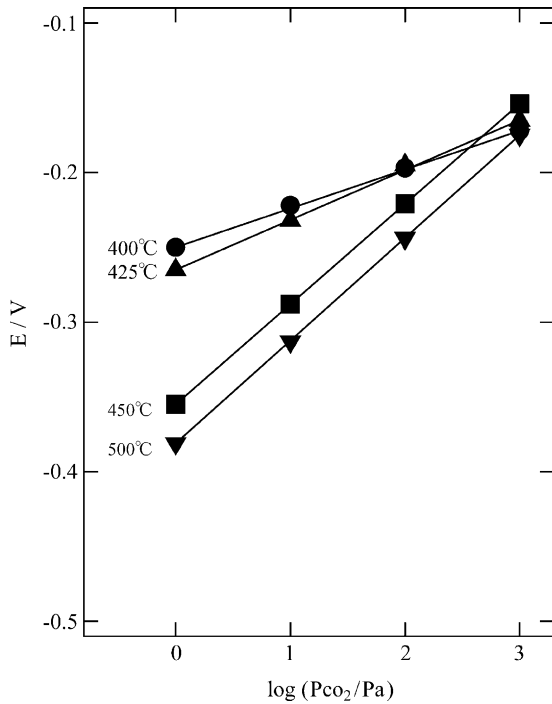


Fig. 9. Dependence of sensor EMF on CO<sub>2</sub> partial pressure: (–) air, Pt[(Na<sub>2</sub>O)<sub>35.7</sub>(Y<sub>2</sub>O<sub>3</sub>)<sub>7.2</sub>(SiO<sub>2</sub>)<sub>57.1</sub> glass|Au, Na<sub>2</sub>CO<sub>3</sub>, CO<sub>2</sub>, O<sub>2</sub> (+).

to an atmosphere of  $2.1 \times 10^4$  Pa oxygen partial pressure, so that the electrode reaction can be expressed by the following equation.

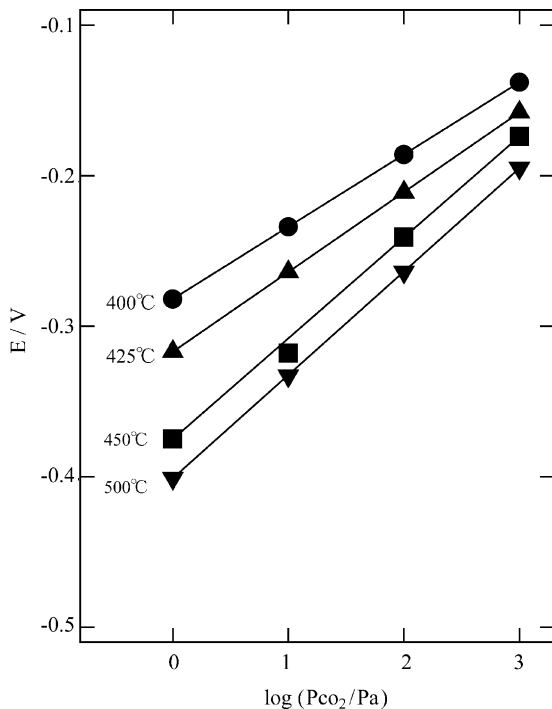
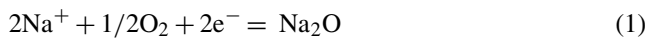
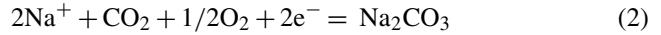


Fig. 10. Dependence of sensor EMF on CO<sub>2</sub> partial pressure: (–) air, Pt[(Na<sub>2</sub>O)<sub>35.7</sub>(Y<sub>2</sub>O<sub>3</sub>)<sub>7.2</sub>(SiO<sub>2</sub>)<sub>57.1</sub> ceramic|Au, Na<sub>2</sub>CO<sub>3</sub>, CO<sub>2</sub>, O<sub>2</sub> (+).

And the reaction at the detection electrode is assumed as follows.



When the Nernst's equation is applied to the above Eqs. (1) and (2), the potentials of counter electrode,  $E_c$ , and the detection electrode,  $E_s$ , can be expressed by the Eqs. (3) and (4), respectively:

$$E_c = E'_c - \left( \frac{RT}{2F} \right) \ln \left( \frac{a_{\text{Na}_2\text{O}}}{a_{\text{Na}^+}^2 (P_{\text{O}_2}^I)^{1/2}} \right) \quad (3)$$

$$E_s = E'_s - \left( \frac{RT}{2F} \right) \ln \left( \frac{a_{\text{Na}_2\text{CO}_3}}{a_{\text{Na}^+}^2 (P_{\text{O}_2}^{II})^{1/2} P_{\text{CO}_2}} \right) \quad (4)$$

where  $E'$ ,  $R$ ,  $T$ ,  $F$ ,  $a_{\text{Na}_2\text{CO}_3}$ ,  $a_{\text{Na}_2\text{O}}$ ,  $P_{\text{CO}_2}$  and  $P_{\text{O}_2}$  are standard electrode potential, gas constant, absolute temperature, Faraday constant, activities of Na<sub>2</sub>CO<sub>3</sub> and Na<sub>2</sub>O, and partial pressures of CO<sub>2</sub> and O<sub>2</sub>, respectively. As both  $E'_c$  and  $E'_s$  are constants, the EMF abbreviated as  $E$  can be expressed as follows:

$$E = E_s - E_c = E' - \left( \frac{RT}{2F} \right) \ln \left( \frac{a_{\text{Na}_2\text{CO}_3} (P_{\text{O}_2}^I)^{1/2}}{a_{\text{Na}_2\text{O}} P_{\text{CO}_2} (P_{\text{O}_2}^{II})^{1/2}} \right) \quad (5)$$

where  $E'$  is a constant. When  $a_{\text{Na}_2\text{CO}_3}$ ,  $a_{\text{Na}_2\text{O}}$ ,  $P_{\text{O}_2}^I$  and  $P_{\text{O}_2}^{II}$  are kept constant, the CO<sub>2</sub> concentration can be calculated from  $E$ . Undoubtedly, the present results can be rationalized by this Eq. (5).

#### 4. Conclusions

Sodium rare earth silicate glasses and ceramics, (Na<sub>2</sub>O)<sub>35.7</sub>(RE<sub>2</sub>O<sub>3</sub>)<sub>7.2</sub>(SiO<sub>2</sub>)<sub>57.1</sub> (RE = Y, Sm, Gd, Dy, Ho, Er and Yb), were prepared by mixing Na<sub>2</sub>CO<sub>3</sub>, RE<sub>2</sub>O<sub>3</sub> and SiO<sub>2</sub>, and their electrical properties including the potentiometric CO<sub>2</sub> gas sensor responses were investigated. The densities of glasses were 0.2–0.41 g cm<sup>-3</sup> higher than those of the corresponding ceramics and were in fairly good agreement with the theoretical densities predicted for Na<sub>5</sub>RESi<sub>4</sub>O<sub>12</sub> ceramics. For the glass samples, the crystallization temperature and melting temperature of the crystal linearly decreased with increasing ionic radius of RE<sup>3+</sup>, whereas the glass transition temperature was constant regardless of the ionic size. The <sup>23</sup>Na NMR spectral measurement of (Na<sub>2</sub>O)<sub>35.7</sub>(Y<sub>2</sub>O<sub>3</sub>)<sub>7.2</sub>(SiO<sub>2</sub>)<sub>57.1</sub> revealed that there are at least three distinguishable Na<sup>3+</sup>-sites in the ceramic, while all of the Na<sup>3+</sup>-sites are statistically equivalent in the glass. The conductivities of ceramics are one to three orders higher than those of glasses. The conductivities of both glasses and ceramics slightly decreased with increasing the ionic radius of RE<sup>3+</sup> and the highest conductivity was achieved for the Yb samples with the smallest ion radius

of RE<sup>3+</sup>. The dependence of EMF on the logarithm of CO<sub>2</sub> partial pressure for the potentiometric CO<sub>2</sub> gas sensors using (Na<sub>2</sub>O)<sub>35.7</sub>(Y<sub>2</sub>O<sub>3</sub>)<sub>7.2</sub>(SiO<sub>2</sub>)<sub>57.1</sub> glass and ceramic obeyed the Nernst's equation in the temperature range of 400–500 °C and the number of electron transferred can be approximated to 2 above 450 °C. The response characteristics of the sensor were not influenced by the type of solid electrolyte.

### Acknowledgment

This work has been supported by the Advanced Research and Technology Center in Niihama National College of Technology.

### References

- Okuyama, R., Nakashima, H., Sano, T. and Nomura, E., The effect of metal sulfides in the cathode on Na/S battery performance. *J. Power Sources*, 2001, **93**, 50–54.
- Nakayama, S. and Sadaoka, Y., Preparation of an Na<sub>3</sub>Zr<sub>2</sub>Si<sub>2</sub>PO<sub>12</sub>-sodium aluminosilicate composite and its application as a solid-state electrochemical CO<sub>2</sub> gas sensor. *J. Mater. Chem.*, 1993, **4**, 663–668.
- Miyachi, Y., Sakai, G., Shimanoe, K. and Yamazoe, N., Fabrication of CO<sub>2</sub> sensor using NASICON thick film. *Sens. Actuators B*, 2003, **93**, 250–256.
- Shannon, R. D., Taylor, B. E., Gier, T. E., Chen, H. Y. and Berzins, T., Ionic conductivity in Na<sub>5</sub>YSi<sub>4</sub>O<sub>12</sub>-type silicates. *Inorg. Chem.*, 1978, **17**, 958–964.
- Asahi, T., Kamata, S., Imai, S. and Nakayama, S., Synthesis of Na<sub>2</sub>O–RE<sub>2</sub>O<sub>3</sub>–SiO<sub>2</sub> (RE=Sm, Gd, Dy, Y, Ho, Er and Yb) system glasses and their electrical properties. *J. Ceram. Soc. Jpn.*, 2000, **108**, 774–776.
- Nakayama, S., Asahi, T., Aung, Y. L., Ohhara, R. and Sakamoto, M., Electrical properties of (K<sub>2</sub>O)<sub>35.7</sub>(RE<sub>2</sub>O<sub>3</sub>)<sub>7.2</sub>(SiO<sub>2</sub>)<sub>57.1</sub> (RE = Sm, Gd, Dy, Y, Ho, Er, Yb) glasses. *J. Ceram. Soc. Jpn.*, 2004, **112**, 238–241.
- Beyeler, H. U. and Hibma, T., The sodium conductivity paths in the superionic conductors Na<sub>5</sub>RESi<sub>4</sub>O<sub>12</sub>. *Solid State Commun.*, 1978, **27**, 641–643.
- Lee, F. C., Marr, J. and Glasser, F. P., Compounds in the Na<sub>2</sub>O–Y<sub>2</sub>O<sub>3</sub>–SiO<sub>2</sub> system. *Ceram. Int.*, 1981, **7**, 43–47.
- Alexander, M. G. and Riley, B., Ion conducting glasses in the Na<sub>2</sub>O–Y<sub>2</sub>O<sub>3</sub>–SiO<sub>2</sub> and Li<sub>2</sub>O–Y<sub>2</sub>O<sub>3</sub>–SiO<sub>2</sub> systems. *Solid State Ionics*, 1986, **18/19**, 478–482.
- Alexander, M. G., Effect of modifier cation on Na<sup>+</sup> conductivity in sodium silicate glasses. *Solid State Ionics*, 1987, **22**, 257–260.
- Hakim, R. M. and Uhlmann, D. R., Electrical conductivity of alkali silicate glasses. *Phys. Chem. Glass*, 1971, **12**, 132–138.